



Published in final edited form as:

*Invest Radiol.* 2018 April ; 53(4): 229–235. doi:10.1097/RLI.0000000000000433.

## Potential of Non-contrast MRI with Diffusion Weighted Imaging in characterization of breast lesions: Intra-individual Comparison with Dynamic Contrast-Enhanced Magnetic Resonance Imaging

Pascal A.T. Baltzer<sup>1</sup>, Hubert Bickel<sup>1</sup>, Claudio Spick<sup>1</sup>, Georg Wengert<sup>1</sup>, Ramona Woitek<sup>1</sup>, Panagiotis Kapetas<sup>1</sup>, Paola Clauser<sup>1</sup>, Thomas H. Helbich<sup>1</sup>, Katja Pinker<sup>2</sup>

<sup>1</sup>Department of Biomedical Imaging and Image-guided Therapy, Medical University of Vienna, Währinger Gürtel 18-20 1090 Vienna, Austria.

<sup>2</sup>Department of Radiology, Memorial Sloan-Kettering Cancer Center, 1275 York Avenue, New York, NY, 10065, USA.

### Abstract

**Objectives:** To assess the potential of non-contrast Magnetic Resonances imaging (NC-MRI) with diffusion weighted imaging in characterization of breast lesions in comparison to dynamic contrast-enhanced MRI (DCE-MRI) at 3 Tesla.

**Materials and Methods:** Consecutive patients with conventional imaging (MG, US) BI-RADS 4/5 findings were included in this IRB-approved single-center study. All underwent 3T breast MRI including readout-segmented DWI (rsDWI), Dynamic-Contrast-Enhanced (DCE) and T2w sequences. Final diagnosis was defined by histopathology or follow-up (>24 months). Two experienced radiologists (R1, R2) independently assigned lesion conspicuity (0=minimal to 3=excellent) and BI-RADS scores to NC-MRI (rsDWI including ADC maps) and DCE-MRI (DCE and T2w). Receiver Operating Characteristics (ROC), kappa statistics and Visual Grading Characteristics (VGC) analysis were applied.

**Results:** 67 malignant and 56 benign lesions were identified in 113 patients (mean age 54+/-14y). Areas under the ROC curves were similar: DCE-MRI: 0.901 (R1), 0.905 (R2); NC-MRI: 0.882 (R1), 0.854 (R2); P>0.05, respectively. Kappa agreement was 0.968 (DCE-MRI) and 0.893 (NC-MRI). VGC analysis revealed superior lesion conspicuity by DCE-MRI (0.661, P<0.001).

**Conclusions:** Diagnostic performance and inter-reader agreement of both NC-MRI and DCE-MRI is high, indicating a potential use of NC-MRI as an alternative to DCE-MRI. However, inferior lesion conspicuity and lower inter-reader agreement of NC-MRI need to be considered.

### Keywords

Breast MRI; Gadolinium-based contrast agents; Non-contrast MRI; abbreviated protocols; Patient management

## Introduction

Dynamic contrast-enhanced breast MRI (DCE-MRI) is the most sensitive method for detection of breast cancer<sup>1-5</sup>. A standard breast MRI protocol comprises a T2-weighted sequence followed by the repetitive acquisition of T1-weighted gradient echo sequences after contrast medium (CM) application.

However, a limitation is the necessity of for intravenous CM injection. With the recent controversy about gadolinium containing contrast agents and current recommendations to use gadolinium based contrast agents only when essential diagnostic information cannot be obtained with unenhanced scans, there is an urgent need for non-contrast imaging methods for breast lesion detection and characterization<sup>6-8</sup>.

An alternative rapid approach obviating the need for CM administration is diffusion weighted imaging (DWI). Measurement of water diffusion by this technique provides quantitative information about tissue microstructure that is useful to distinguish between benign and malignant breast lesions<sup>9</sup>. In clinical practice, DWI is usually interpreted in combination with DCE-MRI to increase the specificity<sup>10-12</sup>. Although DWI images can also be used to detect breast cancer<sup>13,14</sup>, subsequent research on the use of DWI to detect and characterize breast cancer yielded heterogeneous results. Early studies were mainly performed at 1.5T and used basic Echo Planar Imaging (EPI) techniques with differences in sensitivity and specificity exceeding 50% and 30%, respectively<sup>14-22</sup>. Besides variable and often non-consecutive study populations, these variations in diagnostic performance may be explained by the inherent disadvantages of the most commonly used single-shot EPI technique: low spatial resolution, spatial distortions and high susceptibility to artifacts<sup>14,23</sup>. In addition, due to the inherent low spatial resolution an anatomical guidance was necessary and therefore additional T2-weighted (T2w) imaging had to be performed. With the implementation of improved scanning technology such as the development of readout-segmented DWI (rsDWI) sequences, these limitations have been overcome<sup>24,25</sup>.

Therefore, the purpose of this lesion characterization study was to intra-individually compare diagnostic performance, inter-reader agreement and lesion conspicuity of non-contrast Magnetic Resonances imaging (NC-MRI) with rsDWI in breast lesions in comparison to dynamic contrast-enhanced MRI (DCE-MRI) at 3 Tesla.

## Methods

The institutional review board approved this prospective, single-institution study and retrospective data analysis and all patients gave written, informed consent.

### Patients:

Within a seven months period, 119 consecutive patients fulfilling the following inclusion criteria were included: 18 years or older, not pregnant, not breastfeeding, an indication for breast MR imaging due to clinical abnormality or suspicious findings at mammography or breast ultrasound (asymmetric density, n=49; architectural distortion, n=24; or breast mass,

n=46; BI-RADS category 4/5), no previous treatment (such as breast surgery up to 12 months before MRI, neoadjuvant chemotherapy, etc.) and no contraindications to MRI or contrast agents. No patients with suspicious microcalcifications only were included as this was not considered a standard indication for MRI at the time of data acquisition. No high-risk patients were part of the study population as all high-risk screening examinations were conducted on a separate magnet.

If the final imaging assessment was BI-RADS 4 or 5, histopathological diagnosis was obtained by means of image-guided biopsy or surgery. In patients downgraded to BI-RADS 3 after negative MRI results and in patients with a benign histopathological result, imaging follow-up demonstrating a stable lesion diameter over at least 24 months was required. A total of six patients were excluded due to incomplete follow-up. Consequently, the final patient population included 113 patients (mean age  $53.8 \pm 15$  standard deviation years, median 53 years, range 16 – 85 years).

### Magnetic Resonance Imaging protocol

All patients underwent 3T MRI (Siemens Tim Trio) using a dedicated 4-channel breast coil (InVivo, Orlando, FL, USA). The sequence protocol consisted of a readout-segmented Echo Planar Imaging Diffusion weighted sequence (RESOLVE, repetition time (TR) 8000 ms, effective echo time (TE): 59 ms, echo spacing 0.32 ms, field of view 360×202 mm, matrix 172×92 pixels, slice thickness 5 mm, inversion recovery fatsat with inversion time (TI) of 210 ms, b-values 0, 850 s/mm<sup>2</sup>, diffusion acquisition: three-scan trace, 5 readout segments, one average, acquisition time: 2:56 min.), a T2-weighted sequence with fat-saturation (TR: 4800 ms, TE: 61 ms, TI: 230ms., field of view 340mm, matrix 314×320 pixels, 34 slices with 4 mm slice thickness, acquisition time 2:26 min and a dynamic contrast-enhanced high temporal and spatial resolution 3D T1-weighted sequence (time-resolved angiography with stochastic trajectories (TWIST), temporal resolution 13.2s, isotropic voxel size of 1.1 mm, TR 4.75 ms and TE 2.5 ms including baseline and dynamic contrast enhanced scans over an acquisition time of 9 min. 144 slices at a field of view of 330 mm were covered). Gd-DOTA was used as contrast agent (Dotarem®, Guerbet, France), injected intravenously as a bolus (0.1 mmol/kg body weight) at 4 ml/s (power injector: Spectris Solaris EP, Medrad, Pittsburgh, PA, USA), and followed by a 20 ml flush of saline solution.

### Data analysis

Two experienced readers (board certified breast radiologists doing >1000 breast MRI including DWI per year, respectively) trained in different institutions (R1, R2) independently read NC-MRI (comprising low and high b-value DWI images and the ADC maps) and DCE-MRI (comprising dynamic contrast enhanced images and T2w images) and assigned a BI-RADS category per examination<sup>26</sup>, see Figure 1. Both readers were blinded to all additional conventional and prior MR imaging, clinical, follow-up and histopathological data. Diagnostic criteria for malignancy in NC-MRI were low ADC values ( $1.25 \cdot 10^{-3}$  mm<sup>2</sup>/s<sup>23</sup>) as measured by small (3–6 mm<sup>2</sup>) Regions of Interest within the darkest part of the lesion ADC map correlate<sup>27</sup>, heterogeneous internal structure and non-circumscribed margins on DWI images (see Table 1, Figure 2). DCE-MRI criteria were used in accordance with the MRI BI-RADS lexicon (see Table 1, Figure 2). For both readings, unambiguous

suspicious or non-suspicious findings lead to a BI-RADS 5 or 2 category, respectively. A combination of suspicious and non-suspicious findings was assigned BI-RADS 4 if more than one suspicious criterion was fulfilled while BI-RADS 3 was assigned if only one suspicious criterion was present. However, no formal clinical decision rule was used and the readers were free to choose the BI-RADS category they deemed appropriate. E.g. for NC-MRI, a circumscribed lesion with homogeneous internal structure would be assigned BI-RADS 4 or even 5 if the ADC value was very low. Enhancement curve type analysis was done visually using standardized window-center presets of the DICOM viewer. In case of doubt, a small Region of Interest between 3–6 mm<sup>2</sup> was drawn in the most enhancing part of the lesion on early subtractions. No CAD software was used for DCE-MRI analysis. The equivalence of both approaches with each other and CAD methods has been demonstrated previously<sup>28</sup>. Lesion size (maximum diameter), localization and laterality were assessed both on NC-MRI and DCE-MRI datasets. Lesion conspicuity was rated on a 4-point confidence scale (0=minimal, 1=sufficient, 2=good, 3=excellent). Further, BI-RADS lesion type (mass, non-mass) was assessed.

### Statistical analysis

Categorical data were compared using chi-square and kappa statistics. After testing for normal distribution by the Kolmogorov-Smirnoff test, scaled data was analyzed using paired and unpaired t-tests as appropriate. Patient-level diagnostic BI-RADS ratings were analyzed by Receiver Operating Characteristics (ROC) analysis and inter-reader variability (kappa statistics) were calculated for both readers. Reference standard was the final diagnosis as described in the “patients” subsection. Lesion conspicuity was compared between NC-MRI and DCE-MRI using Visual Grading Characteristics (VGC) analysis. In short, VGC plots predefined image criterion ratings (lesion conspicuity in this research) against the method they were obtained by (NC-MRI and CE-MRI in this paper) in a manner analogue to ROC analysis. The resulting image area under the VGC curve is then a single non-parametric and rank-invariant statistical measure of the difference in image quality between the two compared methods<sup>29</sup>. Bland-Altman plot analysis was used to investigate differences between NC-MRI and DCE-MRI lesion size measurements. A significance level of 5% was defined. Results were interpreted considering alpha error accumulation but uncorrected P-values are given in text. Statistical analyses were performed using Medcalc 13.2.2, SPSS 20 and Stata 13.

### Results

Final diagnoses in the included 113 patients were benign in 56 (40.7%) and malignant in 67 (59.3%). Malignant lesions were distributed in as follows: 49 invasive ductal cancer, 5 invasive lobular cancers, 9 ductal carcinoma in situ (DCIS), 3 invasive mucinous carcinoma and one sarcoma). All malignant lesions but 3 who underwent 9G MR-guided vacuum assisted breast biopsy were diagnosed by 14 G US-guided core needle biopsy and subsequent clip marking. All breast cancers were subsequently operated after wire localization. The benign lesions verified by histopathology (n=35, 32 by of 14 G US-guided core needle biopsy, 2 by 9G MR-guided vacuum assisted breast biopsy) comprised of 21 proliferative fibrocystic changes, 7 fibroadenoma or fibroadenomatoid hyperplasia, 3

papilloma, 2 periductal mastitis, 1 phyllodes tumor, 1 radial scar. The latter two, all papillomas and 2 fibroadenomas were afterwards surgically resected. The remaining 21 benign lesions showed stable sizes during imaging follow up over 24 months.

Mean lesion size of benign lesions was 27.9+/-17.3 (SD) mm, median 24 mm, range 6–76 mm. Malignant lesions presented a mean size of 25.3+/-18.7 (SD) mm, median 20 mm, range 5–87 mm. Lesions were classified as mass in 78 (mean size 22.7+/-15.5 (SD) mm, median 19.5 mm, range 5–87 mm) and non-mass like in 35 (mean size 40.9+/-19.8 (SD) mm, median 35 mm, range 14–85 mm) cases. The size differences between benign and malignant lesions were not statistically significant ( $P=0.488$ ) whereas mass lesions were significantly smaller than non-mass like lesions ( $P=0.0002$ ). The limits of agreement estimated by Bland-Altman analysis for size measurements between both methods were -8.7 to 7.8 mm with a mean difference of 0.4 mm, thus excluding a systematic difference between both methods. The limits of agreement were broader in non-mass lesions (-17.6 to 16.1 mm, mean difference -0.8 mm) as compared to mass lesions (-3.1 to 2.6 mm, mean difference -0.3 mm). Both readers assigned an average higher lesion conspicuity score to the DCE-MRI compared to the NC-MRI dataset (area under the VGC curve 0.661,  $P<0.001$ , see Figure 3, Table 2). There was no difference regarding lesion conspicuity of small ( $\leq 20$  mm) and large ( $>20$  mm) lesions,  $P=0.461$ .

ROC analysis (Figure 4) revealed an DCE-MRI area under the curve (AUC) of 0.901 (standard error (SE) 0.030, 95% confidence interval (CI) 0.834 to 0.948) for R1 and 0.905 (SE 0.030, 95% CI 0.839 to 0.951). The AUC of NC-MRI was 0.882 (SE 0.031, 95% CI 0.812 to 0.933) for R1 and 0.854 (SE 0.035, 95% CI 0.778 to 0.911) for R2. The AUCs of all methods and readers did not differ ( $P>0.05$ , respectively). AUCs stratified by lesion size as dichotomized into  $\leq 20$  mm (NC-MRI R1: 0.877, NC-MRI R2: 0.854, DCE-MRI R1: 0.912, DCE-MRI R2: 0.928) and  $>20$  mm (NC-MRI R1: 0.898, NC-MRI R2: 0.872, DCE-MRI R1: 0.875, DCE-MRI R2: 0.875) did not differ ( $P>0.05$ , respectively). Resulting sensitivity and specificity values as well as positive and negative likelihood ratios for both methods and readers are given in table 3. Inter-reader kappa agreement was 0.968 (DCE-MRI) and 0.893 (NC-MRI).

False positive findings on NC-MRI comprised 6 (R1)/7 (R2) proliferative fibrocystic changes, one (R1, R2) fibroadenoma, three (R1, R2) papilloma, one (R1, R2) phyllodes tumor and one (R1, R2) inflammation and two (R1)/three (R2) cases with confirmed long-term stability upon follow-up. Of these lesions, both readers recalled 3 less on DCE-MRI (2 (R1)/3 (R2) with long term stability, one fibroadenoma (R1).

False negative findings on both DCE-MRI and NC-MRI comprised of 3 DCIS (histopathological sizes 57, 30 and 15 mm, two G2, one G1) and one invasive ductal cancer G2 of 10 mm. These lesions were rated as benign/probably benign by both readers on contrast-enhanced MRI while both readers did not identify one of the lesions at all. Additionally, on NC-MRI, two mucinous carcinoma lesions (G2) were false negative and not visualized as lesions at all on DWI images and ADC map.

## Discussion

In this intra-individual comparison study, we demonstrated that unenhanced NC-MRI with rsDWI at 3T can be used for breast cancer detection with a comparable performance to DCE-MRI and almost perfect inter-reader agreement. Although there was a tendency towards lower sensitivity and specificity in NC-MRI, these differences were not significant. Therefore, though DCE-MRI was superior in lesion conspicuity, NC-MRI may be considered as a valid alternative to DCE-MRI in patients unsuitable for contrast agent application.

Though arguably contrast-enhanced breast MRI is the most sensitive method for detection of breast cancer, recent years have uncovered several potential dangers associated in particular with linear gadolinium based contrast agents. Nephrogenic systemic fibrosis associated with gadolinium exposition is a potentially lethal disease, however, it is limited to patients with terminal renal insufficiency in particular in combination with organ (e.g. liver) transplantation. More recently, gadolinium depositions in the brain after gadolinium containing contrast media exposition have been described. While the clinical relevance of these findings is yet unknown<sup>30,31</sup>, this highlights the requirement to reduce or even avoid contrast media where not ultimately necessary. This is already reflected by recommendations of official bodies such as the European medicines Agency (EMA)<sup>32</sup>.

In the light of the increasing awareness of the potential dangers associated with gadolinium based contrast agents, our study adds to the question whether DWI-based imaging might replace DCE-MRI or at least be an alternative in in patients unsuitable for contrast agent application. Currently, all international recommendations still consider the use of gadolinium based contrast agents in the breast as mandatory<sup>33–35</sup>. The most useful application for a fast and unenhanced MRI protocol would be screening in dense breasts, as a screening test should be as simple as possible. Long examination times and the need for contrast agent administration have always precluded the use of breast MRI for screening which is solely recommended for this purpose in a population with a lifetime risk for breast cancer >20%<sup>34,36</sup>. Shortened and less expensive examinations could open the way for MRI as a screening tool in women with dense breasts or an intermediate risk for developing breast cancer, an indication currently under investigation<sup>37</sup>.

Literature on unenhanced breast MRI protocols relying on DWI shows variable results. Prior work showed the diagnostic capability of DWI for diagnosis of breast lesions identified by dynamic contrast-enhanced imaging: a meta-analysis by Dorrius et al. demonstrated pooled sensitivity and specificity values of ADC measurements in lesions localized using DCE-MRI of 89% and 84%, respectively<sup>9</sup>. Our diagnostic accuracy is superior to these reported diagnostic parameters, probably because we used an improved DWI technique and did furthermore assess morphological parameters on DWI images as described in a pilot study of unenhanced MRI in mass lesions only<sup>38</sup>. In contrast to this prior work, we investigated consecutive patients with a defined clinical indication and did not perform lesion selection. Several studies with varying indications, cancer prevalence, field strengths' and technical approaches on NC-MRI have been published recently (<sup>15–22,38</sup> see table 4). Sensitivities showed wide variations between 41.7 and 94% while specificity ranged between 58.4% and



96.9%. We explain these variations by both the heterogeneity of techniques used as well as a lack of standardization regarding image combinations and diagnostic criteria applied to NC-MRI. Study populations were highly heterogeneous and designs varied from case control to non-consecutive cases or the inclusion of specific subgroups such as masses or lesions

2cm, leading to variable rates of cancer prevalence (see Table 4). Of note, the improved sequence design applied in our study demonstrated high diagnostic accuracy although we omitted any additional T2w or STIR imaging in image interpretation but solely relied on raw DWI images for morphological information. Furthermore, inter-reader agreement was excellent and underscores the clinical applicability of NC-MRI. The minor inferiority of NC-MRI as compared to DCE-MRI in this respect may be connected to the higher experience in the established technique, DCE-MRI. The better lesion visualization on contrast enhanced T1w gradient echo images is expected due its inherent higher spatial resolution compared to DWI. However, the inferior lesion conspicuity on NC-MRI did not translate into a significantly lower detection rate of malignant lesions. Furthermore, technical improvements leading to higher spatial resolution and lesion contrast are already conceivable <sup>24</sup>.

As an inclusion criterion for this study was a conventional imaging BI-RADS category 4 or 5 assignment, the significant AUs of both NC-MRI and CE-MRI demonstrate a diagnostic benefit of applying both tests in the investigated setting. We can further estimate the rate of unnecessary biopsies that might have been omitted in case of negative MRI findings: up to 75% using NC-MRI and up to 80% using DCE-MRI. Opposing these numbers are false negative rates of 6% (DCE-MRI) and 9% (NC-MRI). Considering that the false negative findings comprised of 3 DCIS and three invasive cancer lesions, two of them invasive mucinous cancer lesions that were exclusively missed by NC-MRI, a black-and-white interpretation precluding any biopsy in MRI negative results is not appropriate. However, DCIS regularly present as microcalcifications and the lower sensitivity of MRI in lesions presenting as microcalcifications has recently been demonstrated <sup>39</sup>. Consequently, a negative MRI should not be used to downgrade clearly suspicious microcalcifications. Further, DWI is prone to miss mucinous carcinoma that present with large collections of extracellular fluid <sup>40</sup>. While the current study thus generally supports the applicability of DWI to downgrade BI-RADS 4 lesions, DCE-MRI seems to be better suited to this purpose due to a lower number of invasive FN findings. Further prospective data in a higher number of patients is required to assess whether BI-RADS benchmarks could be fulfilled by NC-MRI.

There are some inherent limitations of this study: prevalence of malignant lesions and lesion sizes were rather high. This was because no high-risk screening was performed on our 3T magnet and the exclusive investigation of BI-RADS 4 lesions prior to biopsy. Therefore, our patients represent a typical cross-section of a tertiary care assessment center and prevalence of malignancy has been reported similarly high in comparable settings <sup>10,11,15,21</sup>. The rate of pure non-invasive breast cancer was low. This is to be expected in the given setting as DCIS is mainly identified by means of x-ray mammography screening and is not yet considered a routine indication for breast MRI in our institution <sup>39</sup>. Lesions were rather large though also small lesions could be visualized (see Figure 5). Thus, the applicability of our findings in a screening setting is not proven and this particular indication might require additional T2w

sequences<sup>38,19</sup>. While the reproducibility and repeatability of the readout-segmented DWI sequence used in this study has been demonstrated<sup>41</sup>, it needs to be stressed that the applied cut-off for ADC measurements may vary due to scanning technique<sup>9,42</sup>. The choice of b-values was determined by recommendations from prior literature<sup>42</sup>. While these values may allow an adequate calculation of ADC values, higher b-values that are possible with newer scanner generations may allow a better contrast of lesions due to an improved suppression of background tissue signal and thus improve lesion visibility of NC-MRI in the future. In addition, newer techniques such as simultaneous multi-slice DWI may further reduce measurement times, allowing more complex DWI techniques to be implemented in clinical practice<sup>43,44</sup>.

In conclusion, our findings indicate a potential use of NC-MRI as an alternative to DCE-MRI for breast cancer detection as both techniques provide comparable results. These findings are of clinically relevance considering the increasing awareness of potential long-term dangers associated with gadolinium based contrast media and may have considerable impact regarding costs and availability of breast MRI examinations.

## References:

1. Warner E, Messersmith H, Causer P, et al. Systematic review: using magnetic resonance imaging to screen women at high risk for breast cancer. *Ann. Intern. Med* 2008;148(9):671–679. [PubMed: 18458280]
2. Houssami N, Ciatto S, Macaskill P, et al. Accuracy and surgical impact of magnetic resonance imaging in breast cancer staging: systematic review and meta-analysis in detection of multifocal and multicentric cancer. *J. Clin. Oncol. Off. J. Am. Soc. Clin. Oncol* 2008;26(19):3248–3258.
3. Bennani-Baiti B, Bennani-Baiti N, Baltzer PA. Diagnostic Performance of Breast Magnetic Resonance Imaging in Non-Calcified Equivocal Breast Findings: Results from a Systematic Review and Meta-Analysis. *PloS One*. 2016;11(8):e0160346.
4. Kuhl CK. The Changing World of Breast Cancer: A Radiologist's Perspective. *Invest. Radiol* 2015;50(9):615–628. [PubMed: 26083829]
5. Mann RM, Mus RD, van Zelst J, et al. A novel approach to contrast-enhanced breast magnetic resonance imaging for screening: high-resolution ultrafast dynamic imaging. *Invest. Radiol* 2014;49(9):579–585. [PubMed: 24691143]
6. Sadowski EA, Bennett LK, Chan MR, et al. Nephrogenic systemic fibrosis: risk factors and incidence estimation. *Radiology*. 2007;243(1):148–157. [PubMed: 17267695]
7. Errante Y, Cirimele V, Mallio CA, et al. Progressive increase of T1 signal intensity of the dentate nucleus on unenhanced magnetic resonance images is associated with cumulative doses of intravenously administered gadodiamide in patients with normal renal function, suggesting dechelation. *Invest. Radiol* 2014;49(10):685–690. [PubMed: 24872007]
8. Kanda T, Osawa M, Oba H, et al. High Signal Intensity in Dentate Nucleus on Unenhanced T1-weighted MR Images: Association with Linear versus Macrocyclic Gadolinium Chelate Administration. *Radiology*. 2015;275(3):803–809. [PubMed: 25633504]
9. Dorrius MD, Dijkstra H, Oudkerk M, et al. Effect of b value and pre-admission of contrast on diagnostic accuracy of 1.5-T breast DWI: a systematic review and meta-analysis. *Eur. Radiol* 2014;24(11):2835–2847. [PubMed: 25103535]
10. Pinker K, Bickel H, Helbich TH, et al. Combined contrast-enhanced magnetic resonance and diffusion-weighted imaging reading adapted to the “Breast Imaging Reporting and Data System” for multiparametric 3-T imaging of breast lesions. *Eur. Radiol* 2013;23(7):1791–1802. [PubMed: 23504036]
11. Baltzer A, Dietzel M, Kaiser CG, et al. Combined reading of Contrast Enhanced and Diffusion Weighted Magnetic Resonance Imaging by using a simple sum score. *Eur. Radiol* 2015.



12. Partridge SC, DeMartini WB, Kurland BF, et al. Quantitative diffusion-weighted imaging as an adjunct to conventional breast MRI for improved positive predictive value. *AJR Am. J. Roentgenol* 2009;193(6):1716–1722. [PubMed: 19933670]
13. Kuroki-Suzuki S, Kuroki Y, Nasu K, et al. Detecting breast cancer with non-contrast MR imaging: combining diffusion-weighted and STIR imaging. *Magn. Reson. Med. Sci. MRMS Off. J. Jpn. Soc. Magn. Reson. Med* 2007;6(1):21–27.
14. Baltzer PAT, Renz DM, Herrmann K-H, et al. Diffusion-weighted imaging (DWI) in MR mammography (MRM): clinical comparison of echo planar imaging (EPI) and half-Fourier single-shot turbo spin echo (HASTE) diffusion techniques. *Eur. Radiol* 2009;19(7):1612–1620. [PubMed: 19288109]
15. Yabuuchi H, Matsuo Y, Sunami S, et al. Detection of non-palpable breast cancer in asymptomatic women by using unenhanced diffusion-weighted and T2-weighted MR imaging: comparison with mammography and dynamic contrast-enhanced MR imaging. *Eur. Radiol* 2011;21(1):11–17. [PubMed: 20640898]
16. Wu L-M, Chen X-X, Xu J-R, et al. Clinical value of T2-weighted imaging combined with diffusion-weighted imaging in preoperative T staging of urinary bladder cancer: a large-scale, multiobserver prospective study on 3.0-T MRI. *Acad. Radiol* 2013;20(8):939–946. [PubMed: 23746384]
17. Trimboli RM, Verardi N, Cartia F, et al. Breast cancer detection using double reading of unenhanced MRI including T1-weighted, T2-weighted STIR, and diffusion-weighted imaging: a proof of concept study. *AJR Am. J. Roentgenol* 2014;203(3):674–681. [PubMed: 25148175]
18. Telegrafo M, Rella L, Stabile Ianora AA, et al. Unenhanced breast MRI (STIR, T2-weighted TSE, DWIBS): An accurate and alternative strategy for detecting and differentiating breast lesions. *Magn. Reson. Imaging* 2015;33(8):951–955. [PubMed: 26117691]
19. Bickelhaupt S, Laun FB, Tesdorff J, et al. Fast and Noninvasive Characterization of Suspicious Lesions Detected at Breast Cancer X-Ray Screening: Capability of Diffusion-weighted MR Imaging with MIPs. *Radiology*. 2016;278(3):689–697. [PubMed: 26418516]
20. Belli P, Bufi E, Bonatesta A, et al. Unenhanced breast magnetic resonance imaging: detection of breast cancer. *Eur. Rev. Med. Pharmacol. Sci* 2016;20(20):4220–4229. [PubMed: 27831654]
21. Shin HJ, Chae EY, Choi WJ, et al. Diagnostic Performance of Fused Diffusion-Weighted Imaging Using Unenhanced or Postcontrast T1-Weighted MR Imaging in Patients With Breast Cancer. *Medicine (Baltimore)*. 2016;95(17):e3502. [PubMed: 27124054]
22. McDonald ES, Hammersley JA, Chou S-HS, et al. Performance of DWI as a Rapid Unenhanced Technique for Detecting Mammographically Occult Breast Cancer in Elevated-Risk Women With Dense Breasts. *AJR Am. J. Roentgenol* 2016;207(1):205–216. [PubMed: 27077731]
23. Bogner W, Pinker-Domenig K, Bickel H, et al. Readout-segmented echo-planar imaging improves the diagnostic performance of diffusion-weighted MR breast examinations at 3.0 T. *Radiology*. 2012;263(1):64–76. [PubMed: 22438442]
24. Bogner W, Pinker K, Zaric O, et al. Bilateral Diffusion-weighted MR Imaging of Breast Tumors with Submillimeter Resolution Using Readout-segmented Echo-planar Imaging at 7 T. *Radiology*. 2015;274(1):74–84. [PubMed: 25341078]
25. Pinker K, Baltzer P, Bogner W, et al. Multiparametric MR Imaging with High-Resolution Dynamic Contrast-enhanced and Diffusion-weighted Imaging at 7 T Improves the Assessment of Breast Tumors: A Feasibility Study. *Radiology*. 2015:141905.
26. D’Orsi C, Sickles E, Mendelson E, et al. *ACR BI-RADS® Atlas, Breast Imaging Reporting and Data System*. American College of Radiology; 2013.
27. Bickel H, Pinker-Domenig K, Bogner W, et al. Quantitative apparent diffusion coefficient as a noninvasive imaging biomarker for the differentiation of invasive breast cancer and ductal carcinoma in situ. *Invest. Radiol* 2015;50(2):95–100. [PubMed: 25333308]
28. Baltzer PAT, Freiberg C, Beger S, et al. Clinical MR-mammography: are computer-assisted methods superior to visual or manual measurements for curve type analysis? A systematic approach. *Acad. Radiol*. 2009;16(9):1070–1076.

29. Båth M, Månsson LG. Visual grading characteristics (VGC) analysis: a non-parametric rank-invariant statistical method for image quality evaluation. *Br. J. Radiol* 2007;80(951):169–176. [PubMed: 16854962]
30. Runge VM. Safety of the Gadolinium-Based Contrast Agents for Magnetic Resonance Imaging, Focusing in Part on Their Accumulation in the Brain and Especially the Dentate Nucleus. *Invest. Radiol* 2016;51(5):273–279. [PubMed: 26945278]
31. Huckle JE, Altun E, Jay M, et al. Gadolinium Deposition in Humans: When Did We Learn That Gadolinium Was Deposited In Vivo? *Invest. Radiol* 2016;51(4):236–240. [PubMed: 26588463]
32. Anon. European Medicines Agency - Human medicines - Gadolinium-containing contrast agents. Available at: [http://www.ema.europa.eu/ema/index.jsp?curl=pages/medicines/human/referrals/Gadolinium-containing\\_contrast\\_agents/human\\_referral\\_prac\\_000056.jsp&mid=WC0b01ac05805c516f](http://www.ema.europa.eu/ema/index.jsp?curl=pages/medicines/human/referrals/Gadolinium-containing_contrast_agents/human_referral_prac_000056.jsp&mid=WC0b01ac05805c516f). Accessed June 15, 2017.
33. American College of Radiology (ACR). ACR practice parameter for the performance of contrast-enhanced magnetic resonance imaging (MRI) of the breast. 2014. Available at: <http://www.acr.org/~media/2a0eb28eb59041e2825179afb72ef624.pdf>. Accessed October 19, 2015.
34. Sardanelli F, Boetes C, Borisch B, et al. Magnetic resonance imaging of the breast: recommendations from the EUSOMA working group. *Eur. J. Cancer Oxf. Engl.* 1990;26(12):1296–1316.
35. Mann RM, Kuhl CK, Kinkel K, et al. Breast MRI: guidelines from the European Society of Breast Imaging. *Eur. Radiol* 2008;18(7):1307–1318. [PubMed: 18389253]
36. Sardanelli F, Aase HS, Álvarez M, et al. Position paper on screening for breast cancer by the European Society of Breast Imaging (EUSOBI) and 30 national breast radiology bodies from Austria, Belgium, Bosnia and Herzegovina, Bulgaria, Croatia, Czech Republic, Denmark, Estonia, Finland, France, Germany, Greece, Hungary, Iceland, Ireland, Italy, Israel, Lithuania, Moldova, The Netherlands, Norway, Poland, Portugal, Romania, Serbia, Slovakia, Spain, Sweden, Switzerland and Turkey. *Eur. Radiol* 2016.
37. Emaus MJ, Bakker MF, Peeters PHM, et al. MR Imaging as an Additional Screening Modality for the Detection of Breast Cancer in Women Aged 50–75 Years with Extremely Dense Breasts: The DENSE Trial Study Design. *Radiology*. 2015;277(2):527–537. [PubMed: 26110667]
38. Baltzer PAT, Benndorf M, Dietzel M, et al. Sensitivity and specificity of unenhanced MR mammography (DWI combined with T2-weighted TSE imaging, ueMRM) for the differentiation of mass lesions. *Eur. Radiol* 2010;20(5):1101–1110. [PubMed: 19936758]
39. Bennani-Baiti B, Baltzer PA. MR Imaging for Diagnosis of Malignancy in Mammographic Microcalcifications: A Systematic Review and Meta-Analysis. *Radiology*. 2016:161106.
40. Woodhams R, Kakita S, Hata H, et al. Diffusion-weighted imaging of mucinous carcinoma of the breast: evaluation of apparent diffusion coefficient and signal intensity in correlation with histologic findings. *AJR Am. J. Roentgenol* 2009;193(1):260–266. [PubMed: 19542422]
41. Spick C, Bickel H, Pinker K, et al. Diffusion-weighted MRI of breast lesions: a prospective clinical investigation of the quantitative imaging biomarker characteristics of reproducibility, repeatability, and diagnostic accuracy. *NMR Biomed.* 2016;29(10):1445–1453. [PubMed: 27553252]
42. Bogner W, Gruber S, Pinker K, et al. Diffusion-weighted MR for differentiation of breast lesions at 3.0 T: how does selection of diffusion protocols affect diagnosis? *Radiology*. 2009;253(2):341–351. [PubMed: 19703869]
43. Runge VM, Richter JK, Heverhagen JT. Speed in Clinical Magnetic Resonance. *Invest. Radiol*. 2017;52(1):1–17.
44. Iima M, Yano K, Kataoka M, et al. Quantitative non-Gaussian diffusion and intravoxel incoherent motion magnetic resonance imaging: differentiation of malignant and benign breast lesions. *Invest. Radiol* 2015;50(4):205–211. [PubMed: 25260092]

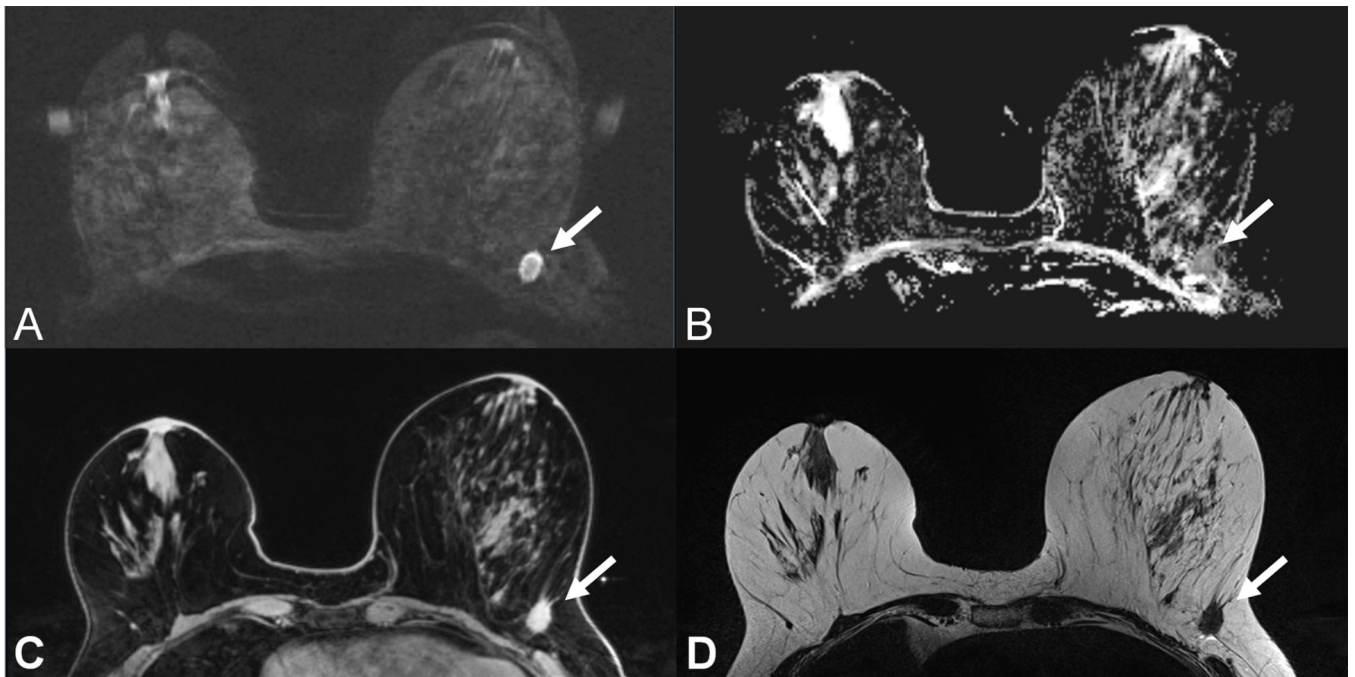


**Figure 1:**

59 year old patient with a T1c invasive ductal cancer G3. Readout-segmented DWI image at  $b=850 \text{ s/mm}^2$  (A) shows ill-defined strongly hyperintense lesion (arrow) with corresponding low Apparent Diffusion Coefficient values on the ADC map (B). Note the similar contrast and morphologic appearance as compared to the T1w contrast enhanced TWIST image (C) and the T2w-TSE image (D).

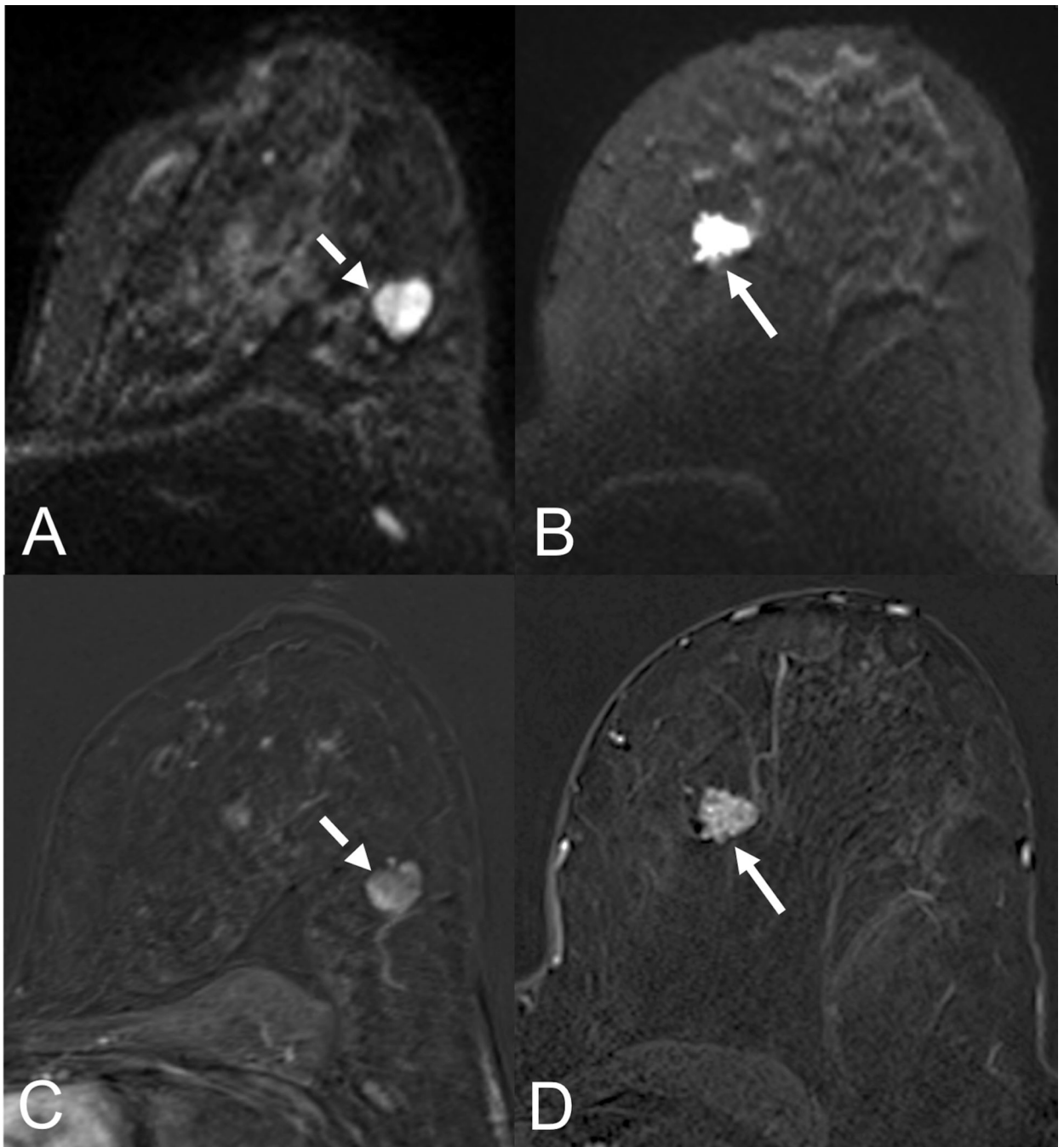


**Figure 2:**

Comparison of morphologic assessment on NC-MRI and CE-MRI. A shows a circumscribed round lesion on the  $b850 \text{ s/mm}^2$  image (dashed arrow) while B visualizes a non-circumscribed, rather spiculated lesion on the  $b850 \text{ s/mm}^2$  image (arrow). The lesion from A appears with circumscribed margins on the early contrast-enhanced subtraction (C, dashed arrow) and was histologically proven as a fibroadenoma while the lesion from B appears non-circumscribed with heterogeneous internal structure and a feeding vessel on the early

contrast-enhanced subtraction (D, arrow) and corresponds to an invasive ductal carcinoma G2.

Author Manuscript

Author Manuscript

Author Manuscript

Author Manuscript

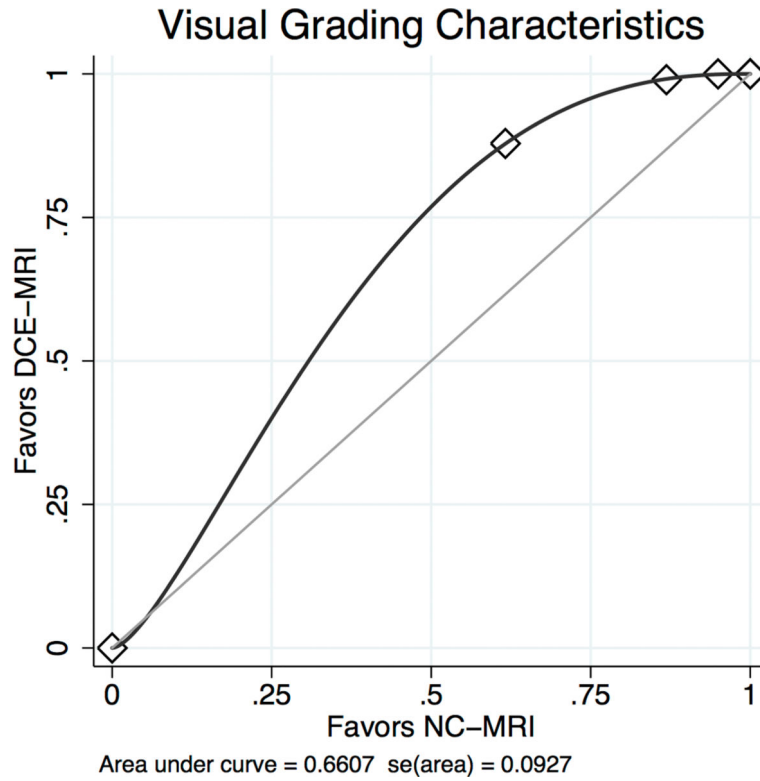


**Figure 3:** Binominal fitted Visual Grading Characteristics (VGC) Curve comparing lesion conspicuity in readout-segmented DWI (NC-MRI) and contrast enhanced MRI (DCE-MRI) reveals an area under the curve of 0.661. The curve significantly ( $P < 0.001$ ) deviates from the null hypothesis (0.5, diagonal line) towards the CE-MRI axis which can be interpreted as a superior lesion conspicuity of CE-MRI compared to NC-MRI.



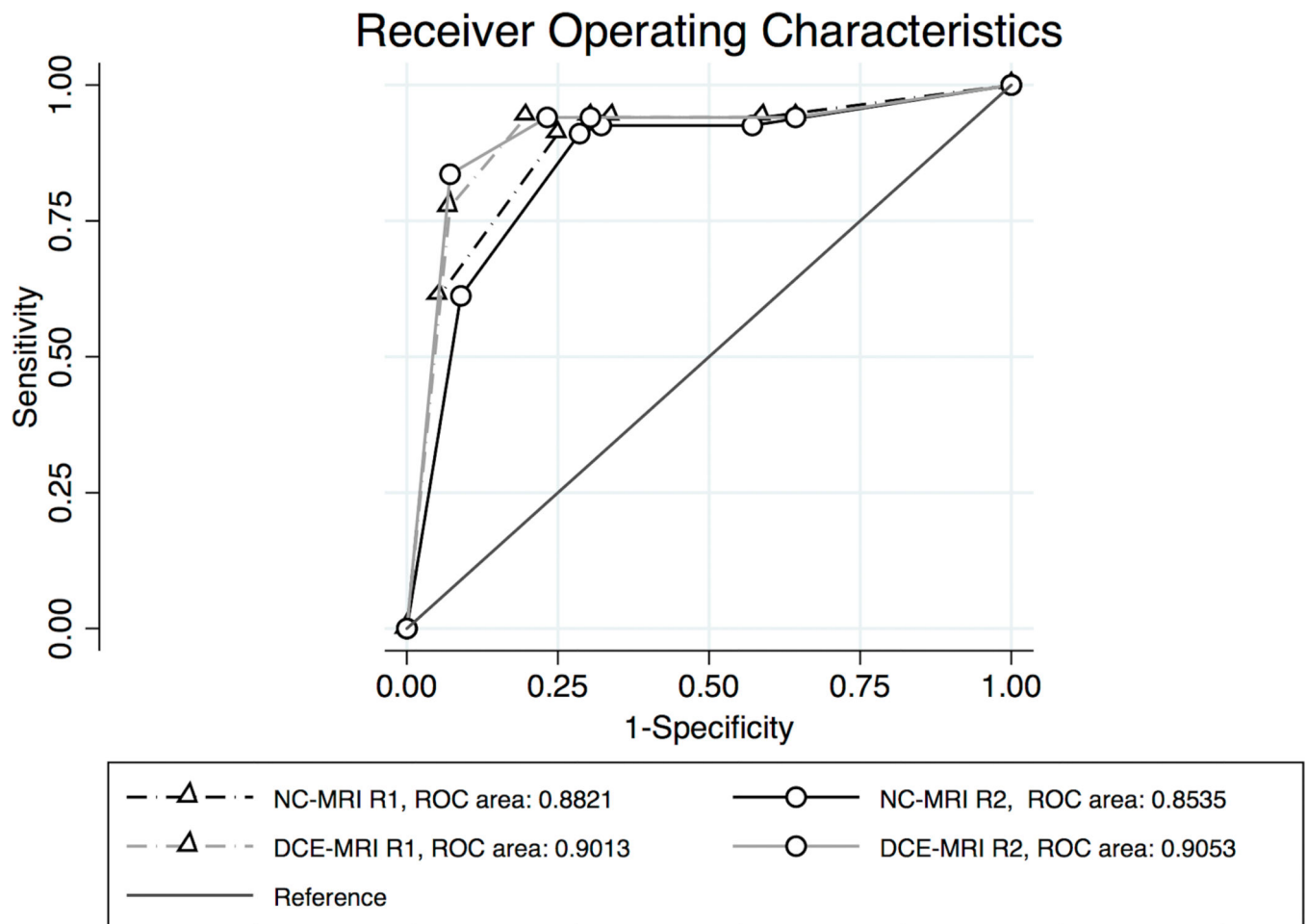


**Figure 4:**  
Receiver Operating Characteristics Curve of BI-RADS ratings for reader 1 (R1) and reader 2 (R2) in readout-segmented DWI (NC-MRI) and contrast enhanced MRI (DCE-MRI).

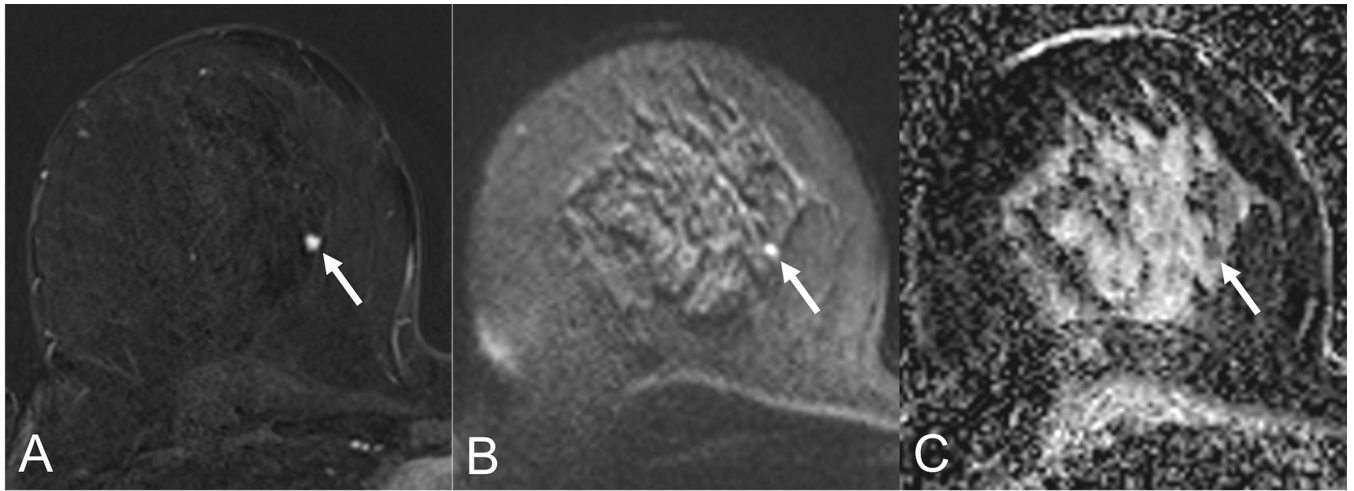


**Figure 5:**

Lesion conspicuity of a small carcinoma (5mm, arrow) in a 53-year old patient. The lesion shows excellent conspicuity on the early contrast-enhanced subtraction (A) while it is adequately visualized on the b850 s/mm<sup>2</sup> image (B). The corresponding ADC map shows a hypointense lesion correlate, corresponding to low ADC-values ( $0.8 \cdot 10^{-3} \text{ mm}^2/\text{s}$ ).

**Table 1:**

Diagnostic criteria for NC-MRI and CE-MRI reading approaches

Method	Criterion	Suspicious	Not suspicious
NC-MRI	ADC	$1.25 \cdot 10^{-3} \text{ mm}^2/\text{s}$	$>1.25 \cdot 10^{-3} \text{ mm}^2/\text{s}$
	Internal structure	Heterogeneous	Homogeneous
	Margins	Not circumscribed	Circumscribed
CE-MRI	Enhancement curve type	Washout, Plateau	Persistent
	Shape (mass)	Irregular	Round, oval
	Margin (mass)	Not circumscribed	Circumscribed
	Internal enhancement (mass)	Heterogeneous, rim	Homogeneous, septations
	Distribution (non-mass)	Segmental, linear	Focal, regional, diffuse
	Internal enhancement (non-mass)	Not homogeneous	Homogeneous

NC-MRI: Non-contrast MRI (readout-segmented DWI), CE-MRI: Contrast-enhanced MRI (DCE-MRI plus T2w), ADC: Apparent Diffusion coefficient

**Table 2:**

Diagnostic parameters for both readers (R1, R2) and reading approaches (NC-MRI, DCE-MRI)

	Sensitivity (TP/TP+FN)	95% CI	Specificity (TN/TN+FN)	95% CI	LR+	95% CI	LR-	95% CI
CE-MRI (R1)	94.0 (64/67)	85.4 – 98.3	80.4 (45/56)	67.6 – 89.8	4.79	2.8 – 8.2	0.074	0.03 – 0.2
CE-MRI (R2)	94.0 (63/67)	85.4 – 98.3	76.8 (43/56)	63.6 – 87.0	4.05	2.5 – 6.5	0.078	0.03 – 0.2
NC-MRI (R1)	91.0 (61/67)	81.5 – 96.6	75.0 (42/56)	61.6 – 85.6	3.64	2.3 – 5.8	0.12	0.05 – 0.3
NC-MRI (R2)	91.0 (61/67)	81.5 – 96.6	71.4 (40/56)	57.8 – 82.7	3.19	2.1 – 4.9	0.13	0.06 – 0.3

NC-MRI: Non-contrast MRI (readout-segmented DWI), CE-MRI: Contrast-enhanced MRI (DCE-MRI plus T2w), TP: true positives, TN: true negatives, FP: false positives, FN: false negatives, CI: confidence interval, LR+: positive likelihood ratio, LR-: negative likelihood ratio, R1: reader one, R2: reader two

Author Manuscript

Author Manuscript

Author Manuscript

Author Manuscript

**Table 3:**

Lesion conspicuity scores tabulated against each other for NC-MRI and CE-MRI

CE-MRI lesion conspicuity	NC-MRI lesion conspicuity			
	Minimal	Sufficient	Good	Excellent
Minimal	0	0	0	0
Sufficient	0	0	1	0
Good	4	1	7	3
Excellent	2	7	22	66

NC-MRI: Non-contrast MRI (readout-segmented DWI), CE-MRI: Contrast-enhanced MRI (DCE-MRI plus T2w)

Author Manuscript

Author Manuscript

Author Manuscript

Author Manuscript

**Table 4:**

Results of prior studies in comparison with own findings ordered by publication date

	<b>Cancer Prevalence</b>	<b>Field strength</b>	<b>NC-MRI technique</b>	<b>Study population</b>	<b>Sensitivity TP/(TP+FN)</b>	<b>Specificity TN/(TN+FP)</b>
Baltzer et al. 2010 <sup>38</sup>	66.6%	1.5T	ssEPI + T2w–TSE	Consecutive BI-RADS 4 and 5 masses	94.4%	85.2%
Yabuuchi et al. 2011 <sup>15</sup>	66.6%	1.5T	ssEPI + T2w STIR and SPAIR	Mixed: asymptomatic breast cancers and control group	50.0%	95.2%
Wu et al. 2014 <sup>16</sup>	44.6%	3T	ssEPI + T2w–TSE	Suspicious lesions 2cm	86–93%	81–94%
Trimboli et al. 2014 <sup>17</sup>	31.9%	1.5T	EPI + T1w–GE + T2w–STIR	Mixed: 46% preoperative staging	78.4%	87.3%
Telegrafo et al. 2015 <sup>18</sup>	62.6%	1.5 T	DWIBS + STIR + T2w–TSE	Mixed: BI-RADS 4 and 5 lesions; patients with positive family history and dense breasts	93.8%	58.4%
Bickelhaupt et al. 2015 <sup>19</sup>	48.0%	1.5 T	DWIBS MIP + T2w TSE and SPAIR	Screening detected BI-RADS 4 and 5 lesions	91.7%	96.2%
Belli et al. 2016 <sup>20</sup>	44.6%	1.5 T	ssEPI + STIR	Mixed: histologically proven cancers and equivocal findings cases	78.8%	96.9%
Shin et al. 2016 <sup>21</sup>	82.9%	3T	rsDWI + T1w–VIBE	Biopsy-proven malignant masses	91.6%	86.4%
McDonald et al. 2016 <sup>22</sup>	25.3%	1.5T, 3T	ssEPI, fs T2w–FSE + non-fs T1w–GRE	Case-control: 50% malignant masses, 50% healthy; all with dense breasts	41.7%	90.1%
This study	59.3%	3T	rsDWI	BI-RADS 4 and 5 lesions after conventional workup	91.0%	71.4–75.0%

NC-MRI: Non-contrast MRI, TP: true positives, TN: true negatives, FP: false positives, FN: false negatives, ssEPI: single-shot Echo Planar Imaging, rsDWI: read-out segmented DWI, DWIBS: Diffusion Weighted Imaging with Body Signal Suppression, usually ssEPI with STIR fat saturation, TSE: Turbo Spin Echo, STIR: Short Tau Inversion Recovery, SPAIR: Spectrally Adiabatic Inversion Recovery, GE: gradient echo, fs: spectral fat saturation